2.2 Experimental Study of Thermocapillary Flow in The Half-Zone Liquid Bridge of Low Prandtl Number Fluid

NASDA Space Utilization Research Center

EXPERIMENTAL STUDY OF THERMOCAPILLARY FLOW IN THE HALF-ZONE LIQUID BRIDGE OF LOW PRANDTL NUMBER FLUID

Satoshi Matsumoto[1], Masahiko Ohtaka [1], Hidesada Natsui [2], Tatsuya Arai [1], and Shinichi Yoda [1]

[1] National Space Development Agency of Japan, 2-1-1, Sengen, Tsukuba, Ibaraki 305-8505, Japan
[2] Advanced Engineering Services Co. Ltd., 1-6-1, Takezono, Tsukuba, Ibaraki 305-0032, Japan

The first and clear experimental evidence for the transition from the steady to the oscillatory flow was presented by the non-contact temperature measurement of a molten tin surface and the surface flow visualization. The experimental study on thermocapillary convection of low Prandtl number fluid was carried out to understand transition behavior to oscillatory flow. The half-zone liquid bridge of molten tin was formed between hot and cold disks in high vacuum chamber (10^{-5} Pa). The three radiation thermometers were used to measure the free surface temperature at a different azimuthal location at the same time. In addition, the temperature distribution at interface between liquid bridge and cold disk was measured by using very fine thermocouples to detect the transition point and to make clear the oscillation mode more precisely.

It can be detected that the steady thermocapillary convection changes to oscillatory under certain condition. The effect of aspect ratio (L/r) on critical Marangoni number is investigated. The critical Marangoni number decreases with increasing the aspect number. This behavior agrees with numerical simulation done by Imaishi *et al.* qualitatively except for region of smaller aspect ration.

The transducer with 3 × 3 LN element was made and checked its sensitivity. The sensor was verified the stability after heat treatment up to 500 °C. which was same as actual thermocapillary experiment. The frequency band of oscillator was selected to get the clear echo signal. The optimal frequency was 6 to 14 MHz wide-band.

The sphericity and surface roughness of Fe-Ni/SB were improved by an appropriate heat treatment technique on Ni plating process and by the organic additives to the Fe plating solution. The Fe plating rate was obtained. It was found that the thickness increased with time linearly. It could be verified that Fe and Ni plated Shirasu-balloons (Fe-Ni/SB) even in ϕ 0.1 mm reflected the ultrasonic.

1. INTRODUCTION

1. Introduction

It is well known that thermocapillary convection changes its flow motion by increasing the control parameters such as temperature difference. In the case of liquid bridge of low Prandtl number fluid, it is numerically predicted that an axisymmetric steady flow transit to asymmetric 3D steady flow. After that, convection becomes oscillatory under certain condition. Namely, the thermocapillary convection of low Prandtl number fluid go through two transition points to become an oscillatory flow. We need to understand the transition mechanism because the oscillatory flow has an undesirable effect on the crystal growth of semiconductors by the floating zone methods, which lead to striations of the dopant in the crystal. The previous studies, in which a half zone liquid bridge have been often used as a model configuration of the floating zone, have shown that flow and temperature fields were governed by dimensionless parameter of Marangoni (*Ma*) or Reynolds (*Re*) number defined as follows:

$$Ma \equiv \frac{|\sigma_T|\Delta T L}{\mu \kappa} \qquad (1\text{-}1),$$

$$Re \equiv \frac{Ma}{Pr} \qquad (1\text{-}2),$$

σ_T is a temperature gradient of surface tension, ΔT is a temperature difference between hot and cold disks, L is a characteristic length of the fluid, μ is dynamic viscosity, α is thermal diffusivity, and Pr is Prandtl number of the fluid. In this study, a radius (a) of the liquid bridge is used as a characteristic length.

In higher Pr number fluids, it was experimentally proved that a transition from axisymmetric steady to 3D oscillatory flow occurs at a critical Marangoni number (Ma_c). On the other hand, it was numerically predicted that thermocapillary flow in a low Pr number had two transition points [1], [2]: That is, transition from axisymmetric to 3D steady will occur at a first bifurcation point (Ma_{c1}), and transition from 3D steady to oscillatory at a second one (Ma_{c2}). The prediction needs to be experimentally proved.

A detail experiment around the bifurcation point, in which even the Ma_{c2} is predicted to be in the order of 10^1 for a Pr=0.01 liquid bridge [3], is required to prove the transition behavior of Marangoni convection. However, many studies have been conducted at a Marangoni number that is far from the Ma_{c2} because those have mainly focused on a contribution to produce a high quality single crystal from a molten metal.

Nakamura et al. [4], [5] measured a surface temperature fluctuation with a thermocouple in a molten silicon column of 10mm in diameter and 10mm in length, and found that a frequency of the fluctuation was 0.1Hz at a temperature difference of 100K. However, the imposed temperature difference was far from the second bifurcation point. Han et al. [6] experimentally investigated thermocapillary convection in a liquid bridge of mercury. Free surface fluctuations were measured by a non-contacted diagnostic system, and they found the Ma_{c2}, detecting it to be 900 with a frequency around 5Hz. Quite recently, Yang and Kou [7] reported the onset point of temperature fluctuation and its frequency (Ma_{c2}=194 and 1.1Hz) of a molten tin column by the contacted diagnostic, *i.e.* J-type thermocouple. However, disturbances on the flow and temperature field are caused by a thermocouple which contacts

with a fluid and a thermocouple often acts as a cold spot which makes it a complicated temperature gradient along a free surface. It should be noted here that there is no successful experiment to verify the transition behavior of thermocapillary flow by a non-contact diagnostic even nearby the Ma_{c2}.

The goal of present study is to understand the transition phenomena of thermocapillary flow by means of an experimental approach and comparative study with the numerical works in this research group.

The experimental efforts began to select a fluid material for a low Pr number liquid bridge in 1998 [8]. The selected material was molten tin of which Pr number is identical with that of molten silicon (Pr=0.01). Therefore, we can directly compare our experimental result with available experimental and numerical results of molten silicon because the identical Pr number means to show the same fluid dynamic behavior. Moreover, molten tin as a test fluid has an experimental advantage in a detection of Ma_{c2} compared to molten silicon. Since the melting point of tin is much lower than that of silicon, there is no need to use an infrared image furnace for melting a tin sample, which was used for a molten silicon experiment [4] and [5], and an electric heater is applicable to melt it. Thus, it is expected that the surface temperature of a molten tin column can be measured by a non-contact diagnostic with relatively low noise level. The high purity iron was selected as solid material to sustain a liquid bridge because of the reason that moderate wettability and low reactivity against molten tin is required for the solid material [8].

On the other hand, the selected test fluid has a thermodynamic disadvantage which the oxygen partial pressure is extremely low at the equilibrium between molten tin and tin oxides (SnO and SnO_2) near the temperatures for the low Pr experiment (about 570-770K), resulting in suppressing the thermocapillary flow by the formation of an oxide film over a surface of the melt. However, in 1999, we have successfully overcome the difficult problem of oxidation over the tin surface [9]. Consideration concerning the surface science of tin led us to design of a unique experiment apparatus where a clean surface of molten tin can be obtained by the Ar^+ ion etching method and sustained under the high vacuum condition (about 10^{-6}Pa) during an experiment. The performances of the experiment apparatus were already confirmed. In 1999, a non-contact measurement technique of the surface temperature has been also developed to detect small amplitude of temperature fluctuation at around the Ma_{c2} [9]. It was also confirmed that the radiation thermometer which is equipped with the PbS photo detector and combined with the attachments to obtain a high signal-to-noise ratio such as CaF_2 optical pass filter and an isotropic graphite panel had the sufficient temperature resolution to detect the Ma_{c2} with high accuracy. It was concluded that those unique considerations and devices undoubtedly lead us to a success of detecting the transition to oscillatory flow of the low Pr fluid without any flow disturbances.

Compared with the conventional transparent fluid used for a high Pr number experiment, a low Pr number fluid has another experimental difficulty: It is impossible to observe an internal flow field for opaqueness of a low Pr fluid. In order to overcome this problem, a novel visualization technique using an ultrasonic transducer with a high heat resistance has been experimentally studied for an internal flow field measurement since 1999 [9]. The visualization technique also requires a development of a unique balloon-like tracer. A critical condition on the Ma_{c1} and a detail structure of oscillatory flow will be clarified by this measurement technique.

The experimental results with molten tin obtained in 2000 are significant for the thermocapillary convection of a low Pr fluid. As predicted in the last issue [9], we have succeeded in detection of the transition to oscillatory flow by the surface temperature

measurement without any flow disturbances. The flow transition was verified by comparison of the experimentally obtained Ma_{c2} and frequency of surface temperature fluctuation with the numerical results, and by a surface flow visualization experiment directly [10]. The effect of the liquid bridge geometry on the Ma_{c2} and oscillation frequency was further investigated and discussed [11]. The following results are described in this study:

(1) Experimental verification of surface temperature measurement (in-house activity)
(2) Detection of transition phenomena to oscillatory flow (in-house activity)
(3) Effect of aspect ratio on the critical condition and flow structure (in-house activity)
(4) Numerical simulation for the specific case (in-house activity, collaboration with Kyushu University)
(5) Development of measuring technique of internal flow field (entrusted to Toshiba Co.)
(6) Development of visualization tracer (collaboration with Kagoshima Prefectural Institute of Industrial Technology and partly entrusted to NTT Advanced Technology Co.)

2. OSCILLATORY THERMOCAPILLARY FLOW OF MOLTEN TIN

2. 1 Experiment

The experimental apparatus is shown in Figs 2-1, 2-2, 2-3 [8,9,10]. It consists of a liquid bridge formation part, a measurement region, a sample supplying system and a sample cleaner. The liquid bridge was formed by sandwiching between a pair of pure iron disk (purity: 99.5%). All experiments were done in the ultra high vacuum conditions, which were under 10^{-5}Pa, to keep clean sample surface and less heat loss of molten tin liquid bridge. The lower disk was cooled by helium gas and the upper disk was heated by an electric resistant heater to impose the temperature difference. The electric heaters were not controlled by PID (Proportional, Integral and Derivative) control to circumvent the temperature hunting phenomena. The temperature difference was gradually increased from around 0K to above the onset. An imposed ΔT was measured with the thermocouples embedded at near the end face of the disks.

Solid tin (purity: 99.999%) is melted in a quartz tube as illustrated in Fig. 2-2. The melt is supplied onto the lower disk *via* the capillary portion (1mm in inner diameter) of the quartz tube where bulk oxide in the crude fluid can be removed. For further purification, Ar^+ ion etching method was applied and the ion gun designed for surface cleaning was installed in the chamber. Surface temperature of the liquid bridge was measured with a radiation thermometer, in which PbS photo detector was installed, mounted on outside of the chamber.

The lower disk was optimized to measure the temperature field of liquid bridge as shown in Fig.2-3. The measurement of temperature field was necessary to understand the oscillatory thermocapillary convection. Because of the motion of temperature field was coincided with the one of oscillatory flow. It has been inserted some ϕ0.3 mm K-type thermocouples (TC) sheathed a stainless steel in these 0.35mm-holes. The top of thermocouples was adjusted the same position as lower disk plane.

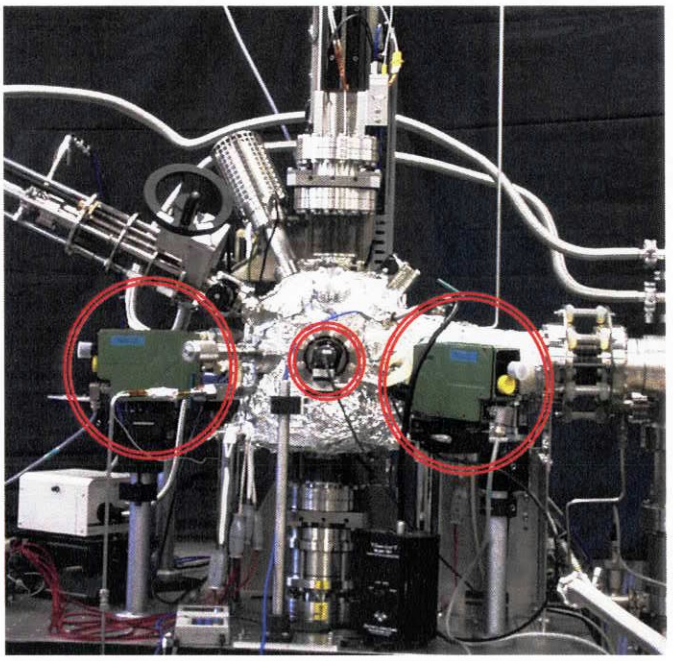

Fig. 2-1 Experimental equipment

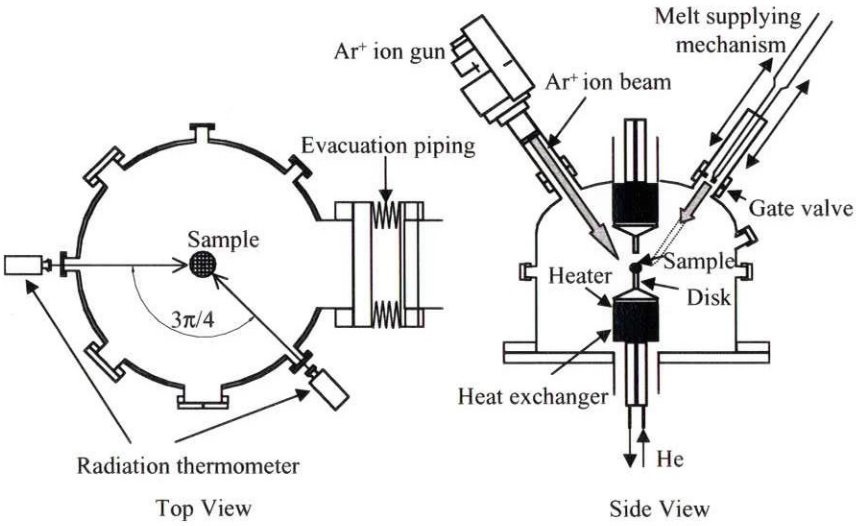

Fig. 2-2 Schematic diagram of experimental equipment

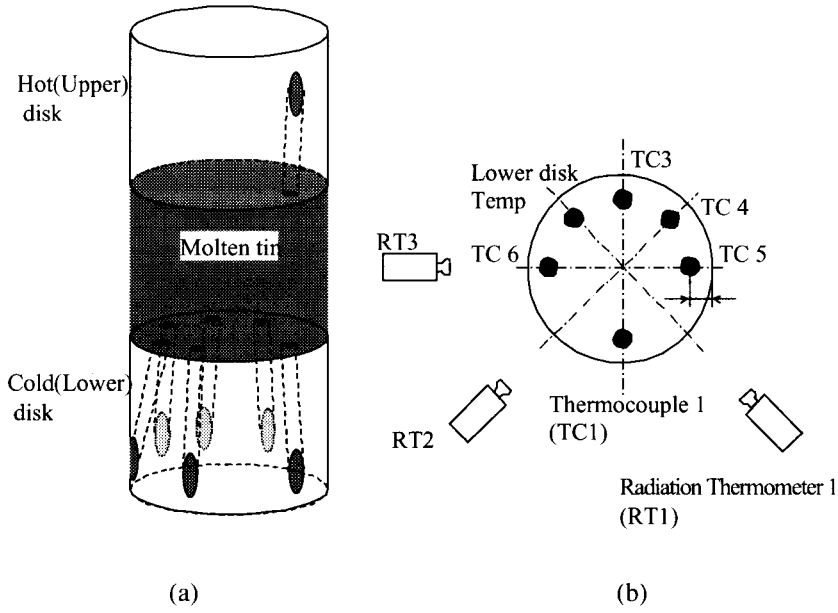

Fig. 2-3 Temperature measurement points
(a) Schematic diagram of tin liquid bridge and disks
(b) Lower disk surface and positions of radiation thermometers

2.2 Detection of Transition Phenomena to Oscillatory Flow

A surface temperature fluctuation of molten tin was successfully observed with the radiation thermometer as shown in Fig. 2-4. The specimen was a liquid bridge of 1.5mm in radius and 2.02 in aspect ratio (As: height/radius). The initial temperatures of the upper and lower disk were 630 and 632K, respectively ($\Delta T = -2K$). The final temperatures of them changed to 616 and 588K, respectively, by the gas cooling of the lower disk ($\Delta T = 28K$). The average changing rate of ΔT ($d\Delta T/dt$) was 0.022K/s. Temperature fluctuations of two points of the liquid bridge surface (measuring area: about 1mm-ϕ) were measured around the center of the bridge height. Since the liquid bridge was slightly deformed by gravity, leading to a difference in radiation energy that can detect by each thermometer, and no correction was made by using the proper emissivity for both thermometers (emissivity: 0.1 for both), absolute temperature values were not the same and not in accord with the real temperature of the liquid bridge. However, it should be noted that the important information is not the absolute temperature but a relative fluctuation component in this study.

The minimum amplitude of the temperature fluctuation was 0.5K in the FFT analysis region as shown in Fig. 2-4-A, which is sufficiently larger than the temperature resolution (0.24K [9]). This fluctuation observed at around 1030sec which corresponded to ΔT=9.1K and Ma=43.3 ($\sigma_T = -0.9\times10^{-4}$ N/mK , $\mu = 1.4\times10^{-3}$ Pas , $\alpha = 2.0\times10^{-5}$ m^2/s). The frequency of the temperature fluctuation was about 0.08Hz near the onset point and then gradually increased (Fig. 2-4-A). In the middle ΔT region, there were some frequency components at around 0.3-0.5Hz (Fig. 2-4-B). After that, the fluctuation behaved as a standing wave of 0.42Hz with a very strong amplitude (Fig. 2-4-C).

It can be concluded that the temperature fluctuations presented here were not caused by external disturbances but caused by the transition to 3D oscillatory Marangoni flow. Validity of the experimentally determined Ma_{c2} and the frequency of the standing wave were

discussed and confirmed by comparing with a numerical result [10].

The present results clearly suggest that the transition to oscillatory Marangoni flow was quantitatively detected by the surface temperature fluctuation measurement. Furthermore, we confirmed the transition by flow visualization with tracking slag movement on the liquid bridge surface. Molten tin pre-mixed with a small amount of the slag particle (tin-oxide) was carefully fed onto the lower rod. Since wettability between the slag and the melt is low and density of the slag is lower than the melt, all the particles exist substantially on the surface near the upper rod at $\Delta T=0$ or less. However, when $+\Delta T$ was imposed, the particles quickly moved down, which showed clearly the existence of downwards flow by Marangoni convection. Figure 2-5 shows the movement of the particles obtained from a video image before and after the onset of the oscillation (a=1.5mm, As=2.29, $d\Delta T/dt = 0.018$ K/s). The upper particles repeated in an oscillatory movement along circumference direction with 0.5 s interval and velocity of about 1.2mm/s. It is concluded that the slag particles moved by pulsating oscillatory thermocapillary flow and that there was an apparent critical ΔT between 7 and 8K. Therefore, the transition was directly verified by this surface flow visualization experiment.

The transition phenomena to oscillatory thermocapillary flow in a low Pr fluid, which has never been observed by a non-contact measurement so far, was successfully detected by those quantitative experiments under normal gravity. However, a liquid bridge geometry in which a gravity effect on thermocapillary flow, especially on a static deformation of the bridge shape, is negligibly small is limited to only a lower height of the bridge (lower than about 2.5mm for a molten tin column) [12]. In the next section, we present the results conducted with the smaller liquid bridges in order to avoid the gravity effect which makes an effect of aspect ratio on the critical condition to oscillatory thermocapillary flow uncertain. It should be noted here that there is a same limitation in a liquid bridge size for a low Pr fluid experiment under normal gravity in general.

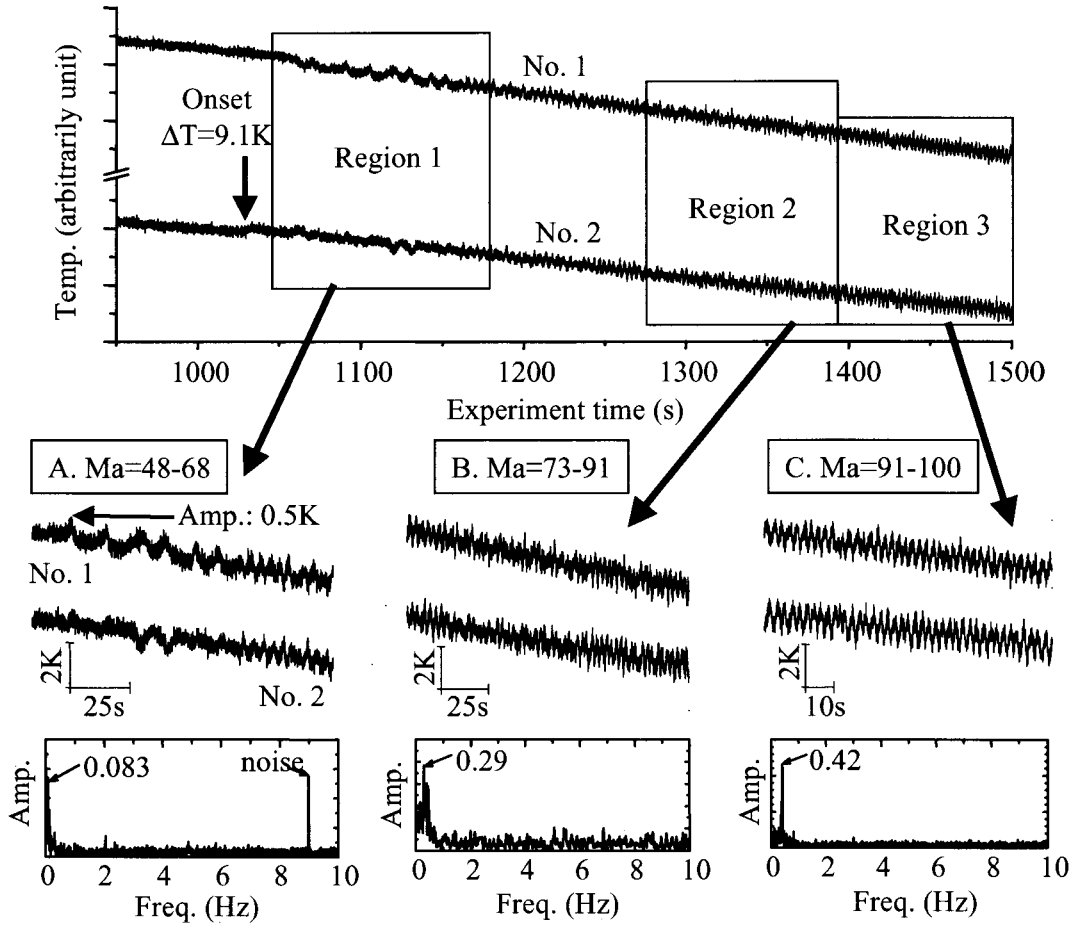

Fig. 2-4 Surface temperature fluctuations of the molten tin column (a=1.5mm, As=2.02). Overall features and enlarged features in A, region 1, B, region 2, and C, region 3 with power spectrum.

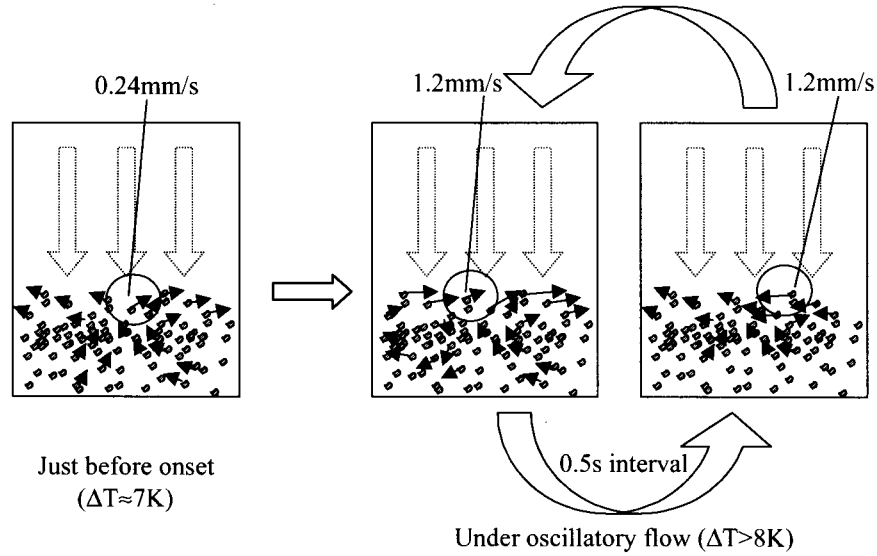

Fig. 2-5 Surface flow visualization by tracking movement of the slag particles before and after the onset of oscillation

2.3 Effects of aspect ratio

(1) Experimental conditions

The disk diameters from 3.0mm to 7.0mm were used in order to covering liquid column with aspect ratio (*As*: height/radius) from 0.8 up to 2.2. This range almost corresponds to calculated range of numerical simulation by Imaishi *et al.* [13]. Heights of the liquid column were adjusted in from 1.5 mm to 4.5 mm at all the experimental cases, minimizing the dynamic bond number *Bd* (*Bd*<1).

$$Bd \equiv \frac{\rho\, g\, \beta\, L^2}{\sigma_T} = \frac{Ra}{Ma}$$

where ρ, is density, g gravitational acceleration, β volumetric expansion coefficient, σ_T temperature gradient of surface tension, L the height of the liquid column and Ra is Rayleigh number. However the static bond number B_0 is larger than unity, volume ratio or diameter ratio (D/D_{max}), surface shape is almost straight.

$$B_0 = \frac{\rho\, g\, L^2}{\sigma}$$

In every case, temperature difference (ΔT) was imposed at certain changing rate. In some cases, ΔT was reduced after transition in order to measure surface temperature behavior when damping. Since the control of changing rate of ΔT (dΔT/dt) is very difficult, there were some widths on them. Influence of dΔT/dt on transition is discussed in (3).

(2) Surface flow patterns

Surface flow visualization at oscillatory flow using fine slag particle (tin-oxide) was performed to investigate influence of *As*. The periodic azimuthally back and forth motion was firstly observed for longer liquid column as shown in previous report [12]. Since the position of movement area was fixed, it was supposed to be pulsating type.

The flow pattern for middle of *As* range showed quite different type. Figure 2-5 shows the rough sketch of the particle movement from video image. A local area, on which slug particles spinning quickly, was appeared at lower of liquid column. It started to repeat azimuthally traveling and turning back motion with some twist angle. After some moment (slightly lager ΔT), this motion change into unidirectional rotation. Much longer liquid column, which *As* was out of experimental range, clearly showed same type of flow pattern as shown Fig. 2-6. A small clean (slug particle less) spot, which was taken place by flow pushing the particles away, was appeared and started similar traveling motion. These local spinning-particle and particle-less areas were supposed to be originated in return flow from cold disk, which was rushed out to surface by transition. Imaishi *et al.* reported similar type of flow pattern and defined this type as "torsion or twisting". This pattern is found over wide range of *As* with certain wave number.

The observed patterns are classified into 3 as follows; 1: azimuthally back and forth motion (position of moving particles is fixed), 2: traveling and turning back motion, and 3: rotation. These patterns are supposed to be corresponded to pulsating, torsion and rotation respectively. It is concluded that the surface flow patterns are qualitatively consistent with one predicted by numerical simulation.

(3) Evaluation of ramping rate

Imaishi *et al.* reported relationship between observation time or ramping rate and Ma_c for relatively higher *Pr* (*Pr*=1). This relationship shows the Ma_c grows exponentially when the fast ramping rate is applied. This work also shows much slower ramping rate is

necessary if larger diameter of liquid column is tested. Since there is no study on them for low *Pr*, appropriate ramping rate needs to be proven.

Following two experiments were performed as shown in Table 2-1. In the experiment No. 1, ramping rate was changed within 5 times of width using liquid column with D = 4mm and *As* was set at almost 1.7. Experiment No. 2 was performed changing D from 4mm up to 7mm with almost constant ramping rate and *As*.

Table 2-1 Experimental conditions for investigating influence of ramping rate

No.	Ramping rate [K/min]	*As*	Diameter of liquid column [mm]
1	0.4 ~ 2.1	1.7	4
2	0.42 ~ 0.6	1	4~7

The Ma_c are plotted against the ramping rate in Fig. 2-7. The almost all data is ranging from *Ma*=100 to 200. The scattering width of *Ma*=100 is mainly supposed to be experimental error. Significant influence of ramping rate (0.5-2 K/min) was not shown for D=4mm. The No.2 experiment was performed in order to investigate influence of the D at constant ramping rate. The D was changed from 4.5mm up to 7mm with fixing *As* 1. An applied ramping rate was about 0.5 K/min, which was slowest ramping rate in No.1 experiment. The Ma_c are plotted against the D in Fig. 2-8. The most data are also ranging from Ma=100 to 200 as No.1 experiment. These results show ramping rate of 0.5 K/min is appropriate as experimental conditions.

(4) Pattern of surface temperature fluctuation

A number of data, which were measured by radiation thermometers, enable us to classify the patterns of surface temperature fluctuation (STF) at the transition into 5 types as follows;

1: Start STF with low* frequency -> Stop STF ->Restart STF with high* frequency
2: Occurrence of temperature shift (one-time) -> No STF -> Start STF with High frequency
3: Start STF with low frequency -> Frequency of STF become higher
4: Start STF with low frequency. After that, frequency of STF become higher with increasing ΔT.
5: Start STF with high frequency
* Definition of frequency speed (order of magnitude); Low: 10^{-2}Hz, High: 10^{-1}Hz

Figure 2-9 also shows rough sketches of the STF for above types. The each type involves several waveforms. Observed wave were periodical waveforms of sinusoidal, triangular, trapezoidal and complex. This suggests that several combination of wave number and oscillation type formed them.

The unknown phenomena such as temperature shift (Type2), the STF with low frequency (Type1, 3 and 4) with once stop STF were observed, but they have not been well understand. However two onsets apparently can be determined in that cases, onset of STF with high frequency is defined as Ma_c in this report.

(5) Ma_c as a function of aspect ratio

In order to clarify Ma_{c2} as a function of As, surface and bottom temperature measurements using liquid columns with As from about 0.8 to 2.2 are carried out.

The Ma_{c2} as a function of As, which was experimentally and numerically obtained by Imaishi *et al.* [13], are shown in Fig. 2-10. The experimental Ma_{c2} in the range of As higher

than about 1.2 well corresponds to numerical one. The experimental Ma_{c2} increases with decreasing of As monotonically. In contrast, the numerical Ma_{c2} has a peak at As=1.2 and the one slightly decreases when As in the range of $1.0 \leq As \leq 1.2$ decreases. The experimental results showed that the Ma_{c2} ($As \leq 1.3$), which was obtained using the liquid column with relative large radius and the one lied on relative low Marangoni number, was obtained by the experimental conditions at small $d\Delta T/dt$. We will make clear the reason why the experimental critical Marangoni number in the smaller aspect region differ from the numerical result in near future.

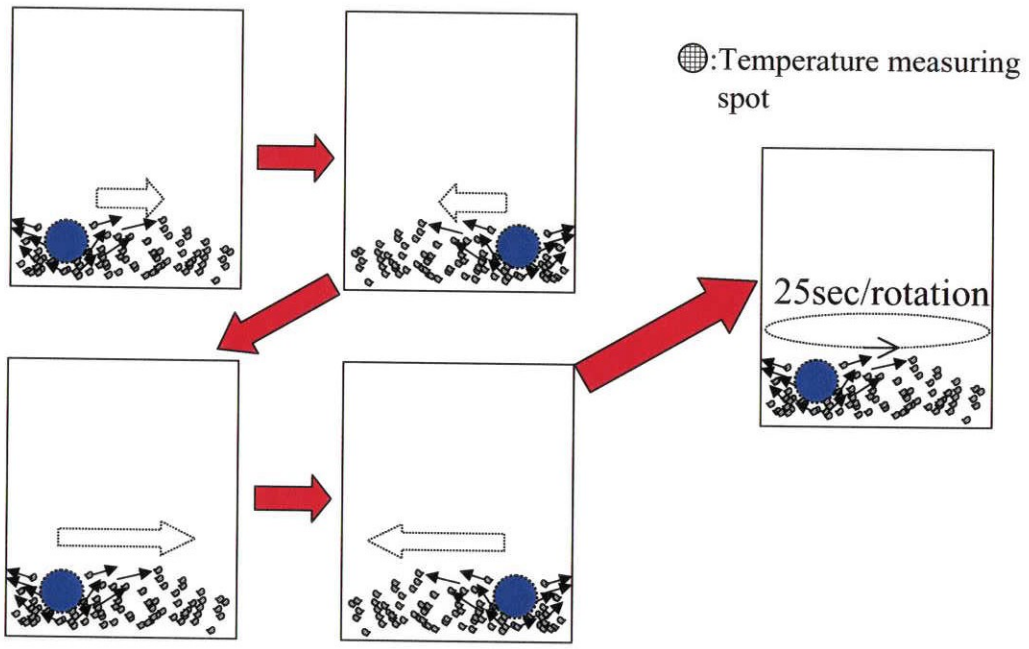

Fig. 2-6 Particle movements taken from video image for higher aspect ratio

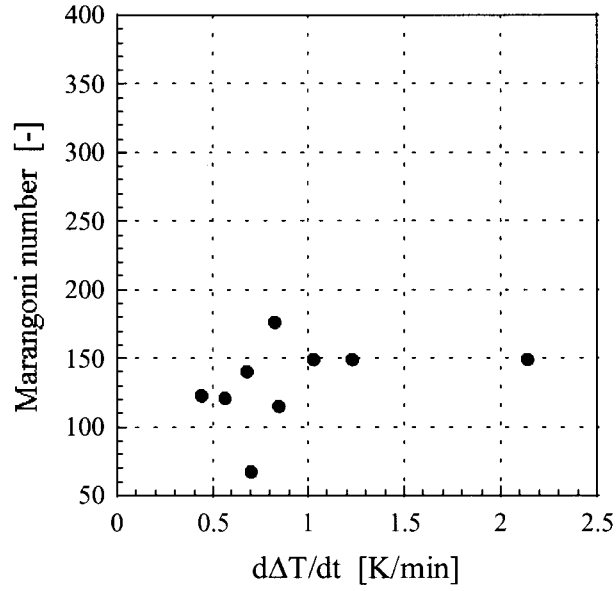

(a) 1.62 < As < 1.78 (D = 4 mm)

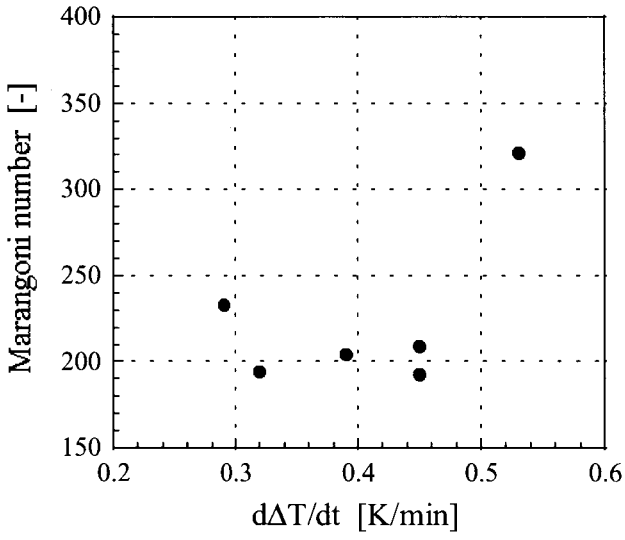

(b) 0.75 < As < 1.10 (D = 7 mm)

Fig. 2-7 Ma_c as a function of ramping rate

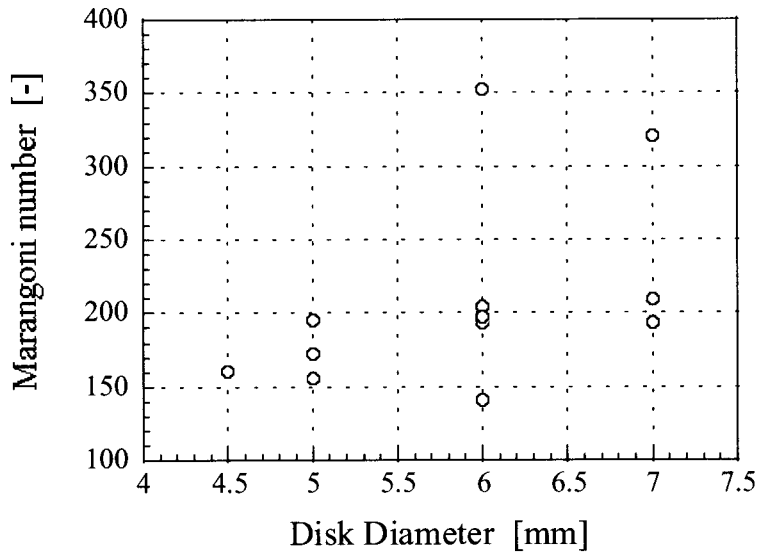

Fig. 2-8 Ma_c as a function of diameter of liquid column
$0.92 < As < 1.09, \quad 0.42 < d\Delta T/dt < 0.6$

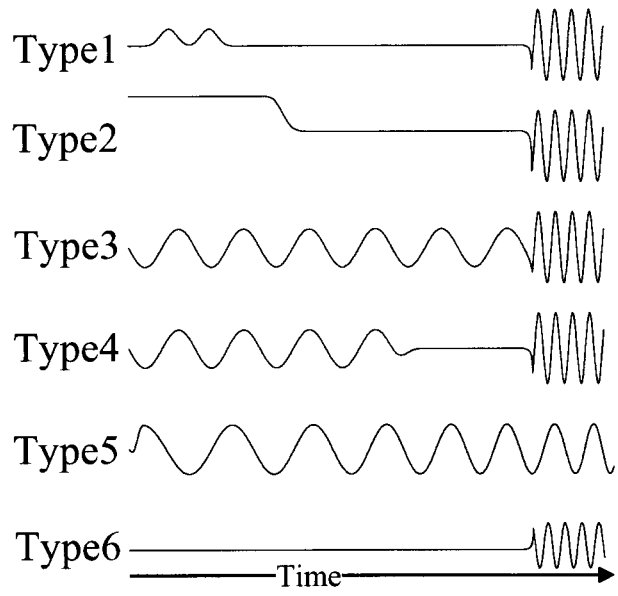

Fig. 2-9 Sketch of patterns of surface temperature fluctuation

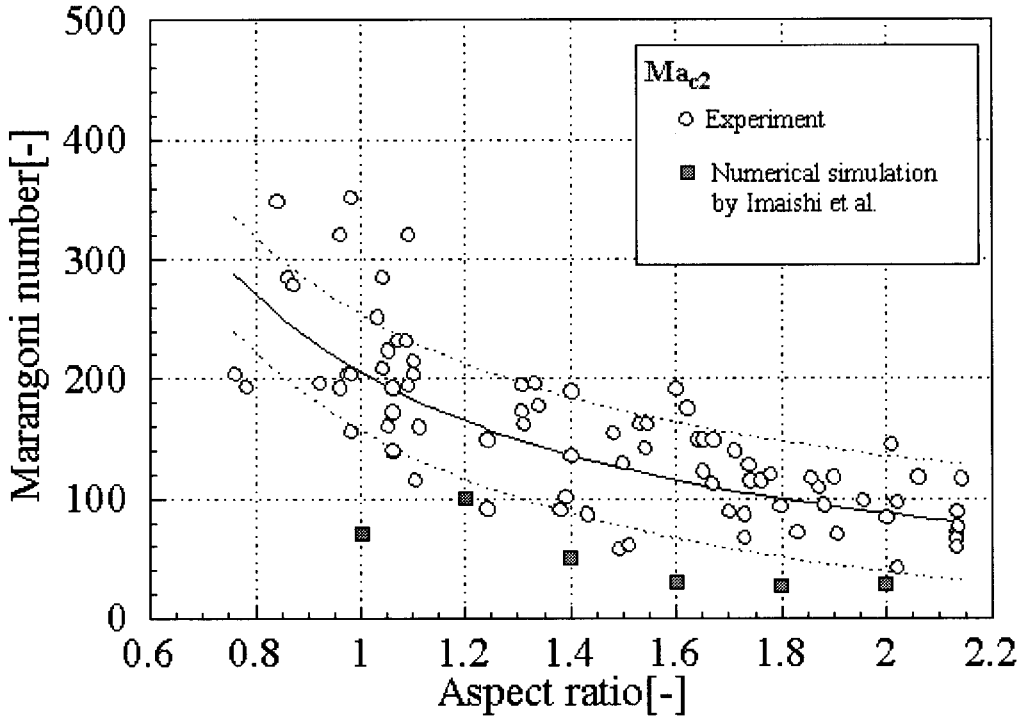

Fig.2-10 Dependence of Marangoni number on aspect ratio

4. DEVELOPMENT OF 3D-UV AND TRACER PARTICLE

4.1 Development of 3D-UV

In 1999, a test for evaluating delectability of $LiNbO_3$(LN) transducer was performed at room temperature using a drilled glass target, which simulated balloon tracers in molten tin. It was predicted that a detectable minimum diameter of tracer was 100-200 μm [9].

In 2000, a test for evaluating sensitivity of transducer at high temperature conditions same as actual thermocapillary experiment was performed in molten tin. High spatial resolution was obtained in the direction of wave propagation. Numerical simulation was performed in order to check visualization performance of ongoing sensor-design. It was confirmed that tracers in molten tin liquid bridge could be visualized.

4.1.1 Making of prototype of UV transducer

The sensor-design was determined by using a numerical simulation and some test until last year. In this development, the prototype of an integrated sensor was made to verify the sensor performance. The $LiNbO_3$ (LN) single crystal as a piezoelectric element was braze on titanium shoe, which is shown Fig. 4-1. Al solder was used to bond the LN element with Ti shoe because this sensor must be endure the high temperature around 450 °C. After brazing, LN plate (6.6 × 6.6 mm) was cut to 3 x 3 matrix element (2.1 × 2.1 mm) by a saw carefully (Fig 4-2). The center of matrix element will not used because the electrical wire cannot lead to it. To recover the senility at a high temperature, the heat treatment carried out after molding the electrodes on the LN element.

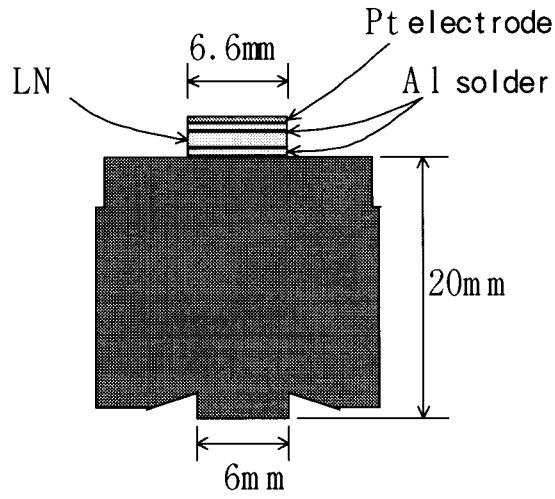

Fig. 4-1 Schematic of shoe with LN element

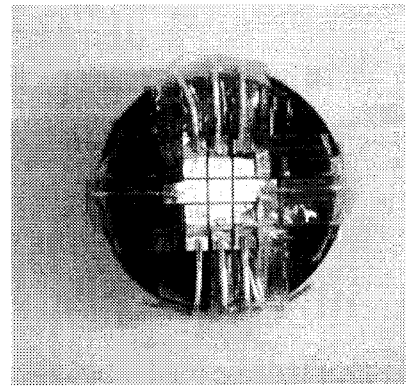

Fig. 4-2 Sensor after cutting

4.1.2 Test of sensitivity

The sensors were checked its sensitivity to compare with both before and after heat treatments. The example of echo signal waveforms is shown in Fig. 4-3. The peaks from edge face of Ti shoe are clearly observed. Echo peak levels are summarized in Table 4-1, which are (a) before heat treatment at room temperature, (b) after heat treatment at 500 °C and (c) after heat treatment at room temperature. The average voltage increased more than 10 % by a heat treatment (compare with (a) and (c) in Table 4-1) and the standard deviation kept almost same. It means that the heat treatment was effective and the sensor was stable with heat up to 500 °C

Table 4-1 Voltage of Echo signal

Matrix No.	11	12	13	21	23	31	32	33	Ave.	S.D.
Condition (a)	0.234	0.367	0.182	0.328	0.395	0.143	0.412	0.260	0.290	0.101
(b)	0.222	0.357	0.183	0.303	0.398	0.147	0.381	0.244	0.279	0.094
(c)	0.232	0.387	0.182	0.393	0.404	0.217	0.438	0.307	0.320	0.099

Unit : [V]
Ave. : Average
S.D. : Standard Deviation

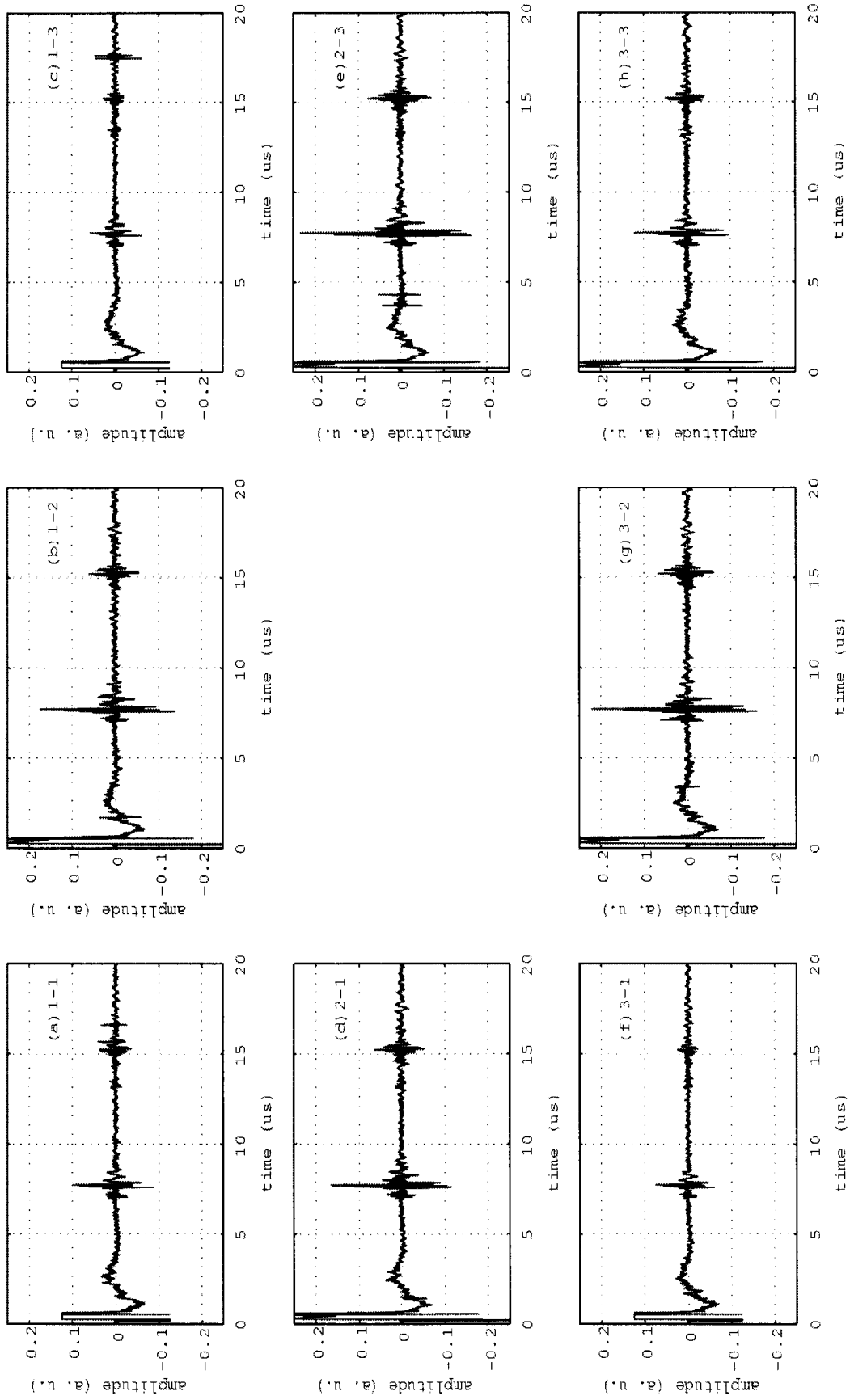

Fig. 4-3 Waveforms of echo signal form edge face of Ti Shoe after heat treatment at 500 °C

4.1.3 Development for 3D-UV Measuring Unit

Ongoing design of 3D-UV measuring unit is briefly described in this section. In this fiscal year, an oscillator/transmitter was made by determining the specification based on previous conceptual investigations.

At first, we discussed the optimal specification of oscillator. The echo form Ti shoe edge was measured by using a breadboard model sensor that consisted of 2 x 2 sensor element. The frequency band was changed to compare a waveform and S/N ratio as follows:

(a) 7 to 25 MHz wide-band
(b) 10 MHz narrow-band (Q=6)
(c) 10 MHz narrow-band (Q=3)
(d) 2.5 to 20 MHz wide-band
(e) 6 to 14 MHz wide-band

The waveform is shown in Fig. 4-4. The amplitude of echo from shoe edge and S/N ratio is shown in Table 4-2. S/N ratio was calculated from peak of S1 divided by noise floor between S1 and S2. In the case of case (e) (6 to 14 MHz wide-band), the echo level of S1 became two times higher than other cases, and the character of waveform was improved because the effect of a low frequency component by a pulsive transmitted signal was disappeared.

As a result, the way to improve the character of waveform although it is difficult to reduce the noise floor in the shoe. Therefore, we selected the frequency band of case (e).

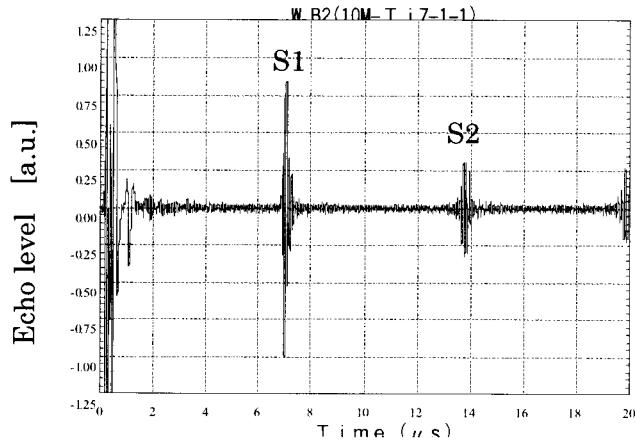

Fig 4-4 Waveform in the case of 6 to 14 MHz wide-band

Table 4-2 Comparison of amplitude of S1 signal and S/N ratio

Frequiecy band	Amplitude of S1	S/N ratio	mark
(a)	47.3 mVp-p	36.3	Good
(b)	15.1 mVp-p	32.1	Not good
(c)	30.6 mVp-p	34.4	Not good
(d)	43.9 mVp-p	35.7	Good
(e)	81.6 mVp-p	36.5	Very good

4.2 Development of Tracer

Fe and Ni plated Shirasu-balloons (Fe-Ni/SB) have been developed for tracers of 3D-UV technique [9]. In 2000, the sphericity and surface roughness of Fe-Ni/SB were improved by an appropriate heat treatment technique on Ni plating process and by the organic additives to the Fe plating solution. The endurance of Fe-Ni/SB against molten tin was examined. It was confirmed that most of tracers were not collapsed but contained in tin melt after the experiment. Acoustic characteristics of Fe-Ni/SB were experimentally studied.

4.2.1 Development of Manufacturing Technique

The sphericity was improved by a apprepriate heat treatment technique on Ni plating process. Figure 4-5 shows Ni plated Sirasu balloons (Ni/SB) before and after the heat treatment. However the shape of Ni plated Sirasu balloons (Ni/SB) was not good sphericity before heat treatment, the one became good sphericity with smooth surface after heat treatment. The detailed technique could not be presented here because patent issue is still pending.

The surface roughness was improved on Fe plating process. The Fe plating layer was formed by an electrolysis plating method. The electrodes were pure iron and carbon. The Ni/SB were stirred with brass balls, which were 2mm in diameter, in a plating solution. The plating solution was consisted of two additives. One was saccharin ($C_7H_5NO_3S$). It absorbs on a cathode and suppresses the growth of projections. The other was sodium dodecyl sulfate ($CH_3(CH_2)_{10}CH_2OSO_3Na$). It was used for a remover of hydrogen gas from the surface of Fe plating layer. The surface roughness of tracers was improved clearly by the additives.

The Fe plating rate was investigated to estimate the plating time in order to get the hopeful tracer particle with appropriate Fe thickness. The time variation of plating thickness is shown in Fig. 4-6. It was found that the thickness increased with time linearly and the plating rate in case of smaller particle was slower than larger one.

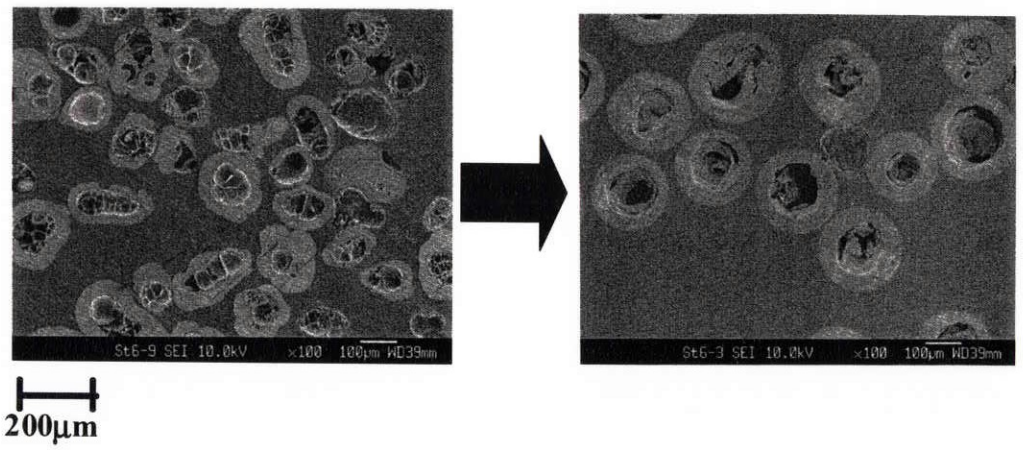

Fig. 4-5 Sphericity of Ni plated Sirasu balloons (Ni/SB) before and after the heat treatment.

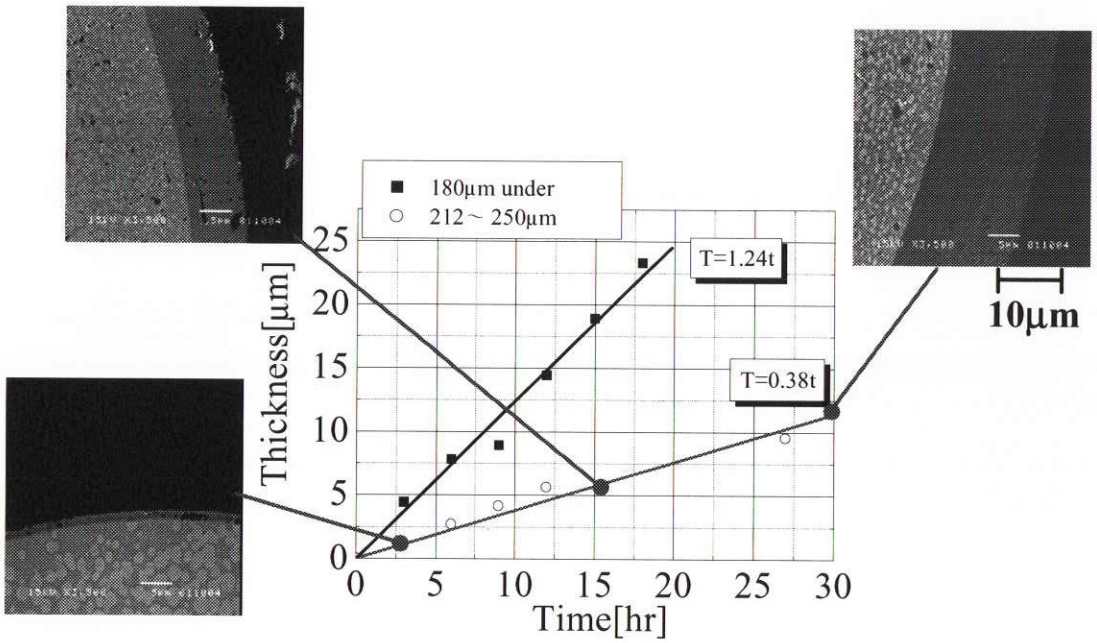

Fig 4-6　Time variation of Fe thickness

4.2.2 Sample for test of detectability

The tracer particle mentioned above was found in a Tin bulk to check the delectability of particle. The position of particle was measured by C-scan probe. Figure 4-7 shows the result of position measurement of both ϕ 1 mm and ϕ 0.1 mm particle. This image was drawn from the strength of echo obtained by scanning the ultrasonic beam on the Tin bulk. It can be verified that Fe and Ni plated Shirasu-balloons (Fe-Ni/SB) even in ϕ 0.1 mm reflected the ultrasonic. The depth of ϕ 1 mm particle was 5 mm from the top and that of ϕ 0.1 mm particle was 6 mm. We will use the Tin bulk with a particle to check the sensitivity of matrix sensors.

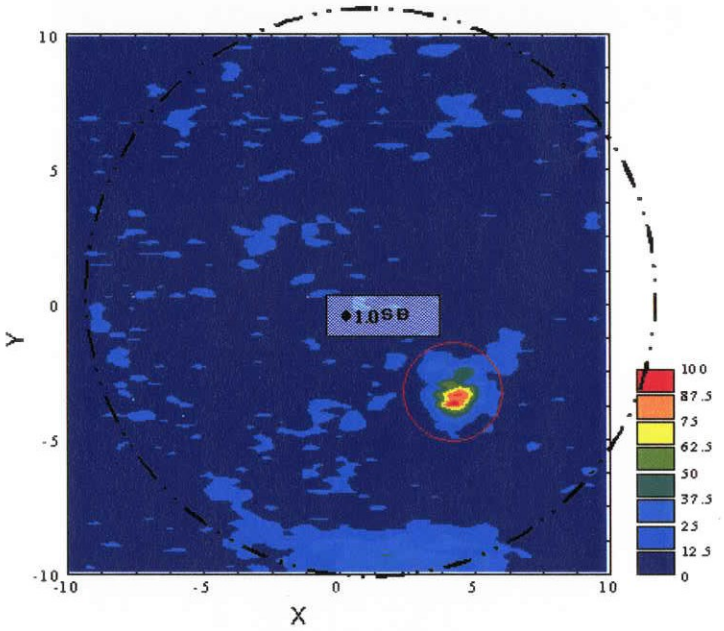

(a) ϕ 1 mm particle

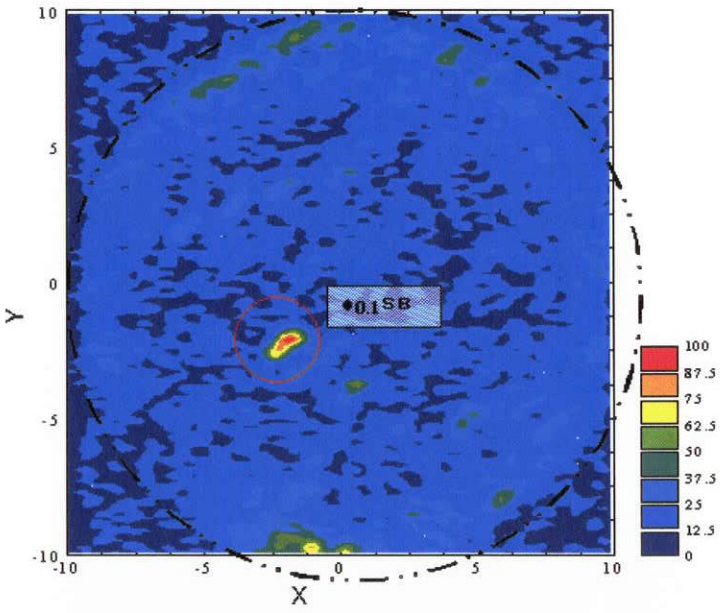

(b) ϕ 0.1 mm particle

Fig. 4-7 Image of echo signal intensity by C-scan probe

5. Conclusions

(1) The experimental study on thermocapillary convection of low Prandtl number fluid was carried out to understand transition behavior to oscillatory flow. The half-zone liquid bridge of molten tin was formed between hot and cold disks in high vacuum chamber (10^{-5} Pa). The three radiation thermometers were used to measure the free surface temperature at a different azimuthal location at the same time. In addition, the temperature distribution at interface between liquid bridge and cold disk was measured by using very fine thermocouples to detect the transition point and to make clear the oscillation mode more precisely.

(2) It can be detected that the steady thermocapillary convection changes to oscillatory under certain condition. The effect of aspect ratio (L/r) on critical Marangoni number is investigated. The critical Marangoni number decreases with increasing the aspect number. This behavior agrees with numerical simulation done by Imaishi *et al.* qualitatively except for region of smaller aspect ration.

(3) The transducer with 3×3 LN element was made and checked its sensitivity. The sensor was verified the stability after heat treatment up to 500 °C. which is same as actual thermocapillary experiment. The frequency band of oscillator was selected to get the clear echo signal. The optimal frequency was 6 to 14 MHz wide-band.

(4) The sphericity and surface roughness of Fe-Ni/SB were improved by an appropriate heat treatment technique on Ni plating process and by the organic additives to the Fe plating solution. The Fe plating rate was obtained. It was found that the thickness increased with time linearly. It could be verified that Fe and Ni plated Shirasu-balloons (Fe-Ni/SB) even in ϕ 0.1 mm reflected the ultrasonic

References

[1] H. Kuhlmann, in: Hydrodynamic Instabilities in Thermocapillary Flows, Microgravity Science Technology VII/2 (1994) 75.

[2] N. Imaishi, S. Yasuhiro, T. Sato, and S. Yoda, in: Proc. 44th SPIE Annual Meeting and Exhibition, Materials Research in Low Gravity II, Denver, **3792** (1999) 344.

[3] N. Imaishi, S. Yasuhiro, and S. Yoda, in: Marangoni Convection Modeling Research Annual Report (NASDA-TMR-000006E), National Space Development Agency of Japan (2000) 157.

[4] S. Nakamura, T. Hibiya, K. Kakimoto, N. Imaishi, S. Nishizawa, A. Hirata, K. Mukai, S. Yoda, and T. Morita, J. Crystal Growth, **186** (1998) 85.

[5] T. Hibiya, S. Nakamura, N. Imaishi, K. Mukai, K. Onuma, P. Dold, A. Cröll, K-W. Benz, and S. Yoda, in: Proc. Joint 1st Pan-Pacific Basin Workshop and 4th Japan-China Workshop on Microgravity Sciences, Tokyo (1998) 8.

[6] J. Han, Z. Sun, L. Dai, J. Xie, and W. Hu, J. Crystal Growth, **169** (1996) 129.

[7] Y.K. Yang and S. Kou, J. Crystal Growth, **222** (2001) 135.

[8] R. Imai, K. Takagi, M. Ohtaka, F. Ohtsubo, H. Natsui, and S. Yoda, in: Marangoni Convection Modeling Research Annual Report (NASDA-TMR-990007E), National Space Development Agency of Japan (1999) 71.

[9] K. Takagi, M. Ohtaka, H. Natsui, T. Arai, and S. Yoda, in: Marangoni Convection

Modeling Research Annual Report (NASDA-TMR-000006E), National Space Development Agency of Japan (2000) 115.
[10] K. Takagi, M. Otaka, H. Natsui, T. Arai, S. Yoda, Z. Yuan, K. Mukai, S. Yasuhiro, and N. Imaishi, J. Crystal Growth, **233** (2001) 399
[11] M. Ohtaka, K. Takagi, H. Natsui, T. Arai, and S. Yoda, in: Proc. 2nd Pan-Pacific Basin Workshop on Microgravity Sciences, Pasadena (2001) IF-1159.
[12] K. Takagi, M. Otaka, H. Natsui, T. Arai, and S. Yoda, J. Jpn. Soc. Microgravity Appl. (in Japanese), **18** (2001) 11.
[13] N. Imaishi, S. Yasuhiro, Y. Akiyama and S. Yoda, J. Crystal Growth, **230** (2001) 164